IMPROVING DIGITAL ROCK PHYSICS PREDICTIVE POTENTIAL FOR RELATIVE PERMEABILITIES FROM EQUIVALENT PORE NETWORKS

Nasiru Idowu[1], Cyril Nardi[1], Haili Long[1], Pål-Eric Øren[1] and Igor Bondino[2]
[1] Lithicon Norway AS, Stiklestadveien 1, 7041 Trondheim, Norway and
[2] Total E&P, Pau, France

This paper was prepared for presentation at the International Symposium of the Society of Core Analysts held in Napa Valley, California, USA, 16-19 September, 2013

ABSTRACT

Both single-phase and multiphase transport properties computed using quasi-static pore network models show sensitivities to the pore network extraction methods. Bondino *et al*. [1] show that differences do exist between predicted single-phase petrophysical properties and relative permeabilities for the same sample as a result of differences in the extracted pore networks from digital rock images. Idowu *et al*. [2] also show that differences do exist in predicted single-phase properties from different pore networks generated from the same sample. Using the same geometrical characterization, they [2] however, show that predicted multiphase transport properties from different pore networks are consistent if the topology of the pore space is well preserved in the extracted skeletons.

In addition to the differences in the predicted transport properties, comparison of water-wet and oil-wet relative permeability trends from Bondino *et al*. [1] and Zhao *et al*. [3] show counter-intuitive trends for some of the pore networks.

Using the same sample as Bondino *et al*. [1] and a quasi-static pore network model, we examine the causes of the apparent differences in the predicted multiphase transport properties and counter-intuitive relative permeability trends. In real porous media, there is no demarcation of the pore space volume to throats and pores but this is required in pore network models. We show that this geometrical characterization/partitioning of pore network elements in general have significant impacts on predicted single-phase and multiphase transport properties. For the networks examined in this study in particular, differences in the predicted single-phase and multiphase properties are caused mainly by the estimated lengths for pores and throats. However, volumes associated with (or allocated to) pores and throats during the pore network extraction processes are responsible for the observed counter-intuitive relative permeability trends.

Finally, we demonstrate an effective method of how some of the uncertainties associated with partitioning of the pore space into pores and throats during pore network extraction processes can be reduced by using $P_c - S_w$ curves computed directly on the grid. This will ensure more representative pore networks even without experimental P_c data.

INTRODUCTION

There are different laboratory techniques and procedures for measuring porosity, absolute permeability, capillary pressure, relative permeability, resistivity index, end-point saturations etc. Appropriate values of these data and other petrophysical properties are assigned to different sections of reservoirs during reservoir characterization, simulations and management. However, depending on the strengths and weaknesses of each method, measurements on the same sample can vary considerably from one technique to another [4, 5]. Similarly, using the same technique and procedures, measurements on the same sample from different laboratories are likely to be different due to human factors and laboratory artefacts [5]. Thus, it is essential to differentiate reliable routine and special core analysis results from highly questionable ones [5].

Digital rock technology (pore-scale imaging and modelling) offers an alternative approach to derive both static and multiphase transport properties from 3D images of rock samples. Similar to laboratory methods, there are several numerical techniques for simulating fluid flow directly on digitised images and predict transport properties. Such techniques include the Lattice Boltzmann method [6], the volume-of-fluid method [7], the level set method [8] and many others [9]. In the same vein, the strengths and weaknesses of each method differ and predicted transport properties on the same sample can also vary considerably. In general, they are all computationally expensive and resolution dependent [9].

Another technique offered by digital rock physics (DRP) is pore network modelling. This approach is computationally efficient with infinite resolution but requires transformation of the irregular and complex geometry of the pore space into a topological and geometrical equivalent network of large pores connected by narrower throats. Using this technique and quasi-static pore network models, several authors [10-12] have demonstrated the predictive capabilities of this approach for sandstones and carbonates.

Extracting pore networks from segmented images involves two main steps: skeletonisation and geometrical characterisation. The skeletonisation process is the generation of topologically equivalent skeletons from voxelized images while geometrical characterization involves partitioning of the network elements into pores and throats and assigning required (geometrical) properties to them. For these two processes, a number of algorithms exist and several combinations are possible [2]. Thus, extracting pore networks is a non-unique process and this raises questions about the predictive power of network models for fluid flow properties.

In this study, we evaluate the causes of the apparent differences in the predicted single-phase petrophysical properties reported in [1, 2]. Secondly, we investigate the causes of the differences in predicted relative permeabilities noted in [1] and counter-intuitive relative permeability trends reported in [1, 3]. Finally, we demonstrate how some of the uncertainties associated with partitioning of the pore space into pores and throats during pore network extraction processes can be reduced and thereby ensuring more representative pore networks.

DESCRIPTION OF SAMPLE AND EXTRACTED PORE NETWORKS

The sample and pore networks used in this section are reported in [1]. For completeness, we summarize the main points below and further details can be found in [1].

- Three samples (S1, S2 and S3) were taken from a small cylindrical end cut of a Clashach sandstone sample with a measured permeability of 1000 mD and porosity of 17%.
- Pore networks were generated using three different network extraction chains (N1, N2 and N3) by two DRP groups.
- DRP group 1 used a Voronoi diagram-based method (N1) with sample S1 to produce S1_N1 network.
- DRP group 2 used a watershed transform approach (N2) with samples S2 and S3 to produce S2_N2 and S3_N2 networks.
- DRP group 2 also used a watershed transform approach with samples S2 and S3 but used the same method as in N1 to define the throat lengths (N3). S2_N3 and S3_N3 networks were produced.
- Table 1 summarises the pore network statistics reported in [1].

Table 1. Pore network statistics showing average coordination number (Z), number of pore (Npores), number of throats (Nthroats), mean throat length to mean throat radius ratio (Th_l / Th_r), percentage of triangular (%TR), square (%SQ), and cylindrical elements (%CL), porosity in fraction (Ø) and absolute permeability (K(mD)) as reported in [1]

		Z	**Npores**	**Nthroats**	**Th_l / Th_r**	**%TR**	**%SQ**	**%CL**	**Ø (frac.)**	**K(mD)**
Group 1	**S1_N1**	3.42	36,446	63,082	8.90	97	3	0	0.16	780
Group 2	**S2_N2**	3.02	49,880	76,611	2.20	65	23	12	0.19	2,456
Group 2	**S2_N3**	3.02	49,880	76,611	11.00	65	23	12	0.19	3,563
Group 2	**S3_N2**	2.00	88,851	89,938	2.23	55	20	25	0.18	1,889
Group 2	**S3_N3**	2.00	88,851	89,938	11.10	55	20	25	0.18	2,504

For simplicity, we will refer to (S2_N2 and S3_N2) and (S2_N3, and S3_N3) networks as _N2 and _N3 networks respectively. For samples S2 and S3, Table 1 shows that the mean throat length to mean throat radius ratios from _N3 networks are roughly 5 times longer than those from _N2. The absolute permeabilities from _N3 networks are also larger.

Other Pore Network Statistics and Properties

When we compare other _N2 and _N3 network parameters for samples S2 and S3, we find that connectivity distributions, throat radius distributions, throat aspect ratios, throat volumes, pore aspect ratios etc. are the same for each sample. Hence, _N2 and _N3 networks are topologically identical and the reported differences in the mean throat length to mean throat radius ratios reported in Table 1 is actually due to differences in throat length distributions since throat radius distribution is exactly the same for _N2 and _N3 networks.

Figure 1 shows a sketch of a throat and its two adjacent pores (denoted *i* and *j*), the distributions of throat length, length of adjacent pores and element length for S1_N1, S2_N2 and S2_N3 networks. An element length is defined as the summation of pore length *i*, throat length and pore length *j* (distance between pore centers of adjacent pores). We observe the following from Figure 1.

- There are differences in the throat length distributions for S2_N2 and S2_N3 networks.
- Lengths of pores (*i* and *j*) are zero in S2_N2 networks and consequently,
- there are large differences in element length distributions for S2_N2 and S2_N3 networks.
- All S1_N1 network statistics and parameters are completely different from those of S2_N2 and S2_N3 networks.

CAUSES OF DIFFERENCES IN PREDICTED RESULTS

Absolute Permeability

The absolute permeability K_{abs}, of a pore network when it is fully saturated with a single phase p of viscosity μ_p is computed from Darcy's law by imposing a constant pressure gradient $\Delta P/L$ across the network and letting the system relax by use of a conjugate gradient method to determine the pore body pressures. The total single phase flow rate q_{sp} is calculated from the pressure distribution. A is the cross-sectional area of the network.

$$K_{abs} = \frac{q_{sp}\mu_p L}{A\Delta P} \qquad \text{eq. (1)}$$

For laminar flow, the flux $q_{p,ij}$ between two adjacent pores *i* and *j* is given by

$$q_{p,ij} = \frac{g_{p,ij}}{L_{ij}}\left(p_{p,i} - p_{p.j}\right) \qquad \text{eq. (2)}$$

where g_p is the fluid conductance, L_{ij} is the element length between the pore centres and p_p is the phase pressure. The fluid conductance g_p for phase p in an irregular triangle is closely approximated by [10]

$$g_p = \frac{3r^2 A}{20\mu_p} \qquad \text{eq. (3)}$$

where r is the radius of the pore or throat. It is apparent from the above equations that differences in the effective length between pore centres of adjacent pores will result in differences in the computed flux $q_{p,ij}$ and hence calculated absolute permeability. The longer the effective length L_{ij} between two adjacent pores the lower the flux $q_{p,ij}$.

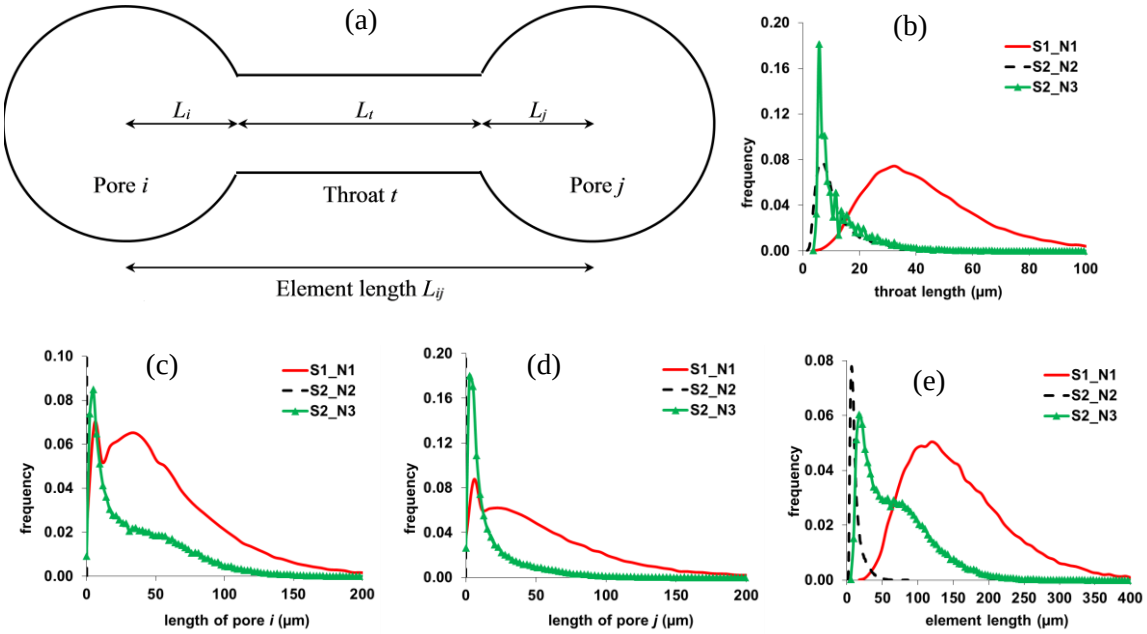

Figure 1: (a) a sketch of throat t with its two adjacent pores (denoted i and j) and comparison of (b) throat length, (c) length of pore i, (d) length of pore j and (e) element length distributions for networks S1_N1, S2_N2 and S2_N3

We recompute the absolute permeability values using our in-house proprietary e-Core code [13] and obtain 785 mD, 2,314 mD, 3,224 mD and 2,408 mD for S1_N1, S2_N2, S2_N3 and S3_N3 respectively. S3_N2 network is unavailable. These results are very comparable to the reported absolute permeability values in Table 1. The mean throat length to mean throat radius ratio from S1_N1 network is approximately 4 times longer than those from _N2 networks and the permeability value is roughly 3 times lower as shown in Table 1. This is the expected trend. However, permeability results for _N2 and _N3 networks show a contrary trend: _N3 networks have mean throat lengths that are roughly 5 times longer than those form _N2 and the permeabilities are still larger for samples S2 and S3.

Are the differences in absolute permeability values between _N2 and _N3 networks and the counter-intuitive trend mainly due to differences in the throat length and pore length (element length) distributions? Since _N2 and _N3 networks have the same number of nodes and throats for each sample, it is possible to change a given parameter distribution for one network to another. We first set pore lengths to zero in S2_N3 as in S2_N2

network. Next, we replace the throat length distribution in S2_N3 with that of S2_N2. This is to ensure that the networks are similar geometrically.

The absolute permeability of S2_N3 network is then recomputed – 2,305 mD. This is approximately the same as S2_N2 network permeability value of 2,314 mD. Replacing the throat length distribution of S2_N2 with that of S2_N3 resulted in similar results: 5,744 mD and 5,698 mD for S2_N2 and S2_N3 respectively.

These values suggest / confirm that the reported differences in permeability in _N2 and _N3 networks are due mainly to differences in throat and pore length distributions. Much lower absolute permeability value of 780 mD for S1_N1 networks compared with others are due to the large differences in the length distributions also as well as the different skeletonization algorithm used (Voronoi diagram-based method).

Other networks parameters that may affect absolute permeability values include throat radius distribution, connectivity, dead-end pores, number of inlet / outlet pores etc. [14]. These parameters are similar and have negligible effects for the networks examined in this study.

Relative Permeability

All network elements in S1_N1 are angular (triangular – 97% and square – 3%), Table 1. This should result in a better connectivity and a higher conductivity of the wetting phase (through wetting films in corners) especially at low wetting phase saturation. However, the published [1] comparison of relative permeability curves shown in Figure 2(a, b and c) shows that S1_N1 has the lowest wetting phase relative permeability (k_{rw}). There are also large variations in k_{rw} compared with slight variations in non-wetting phase relative permeability (k_{rnw}).

We first reproduce the published results as shown in Figure 2 (d, e and f) for primary drainage, imbibition at water-wet and oil-wet conditions. Next, we set pore lengths to zero for both S1_N1 and S2_N3 as in S2_N2 network and re-simulate the different displacement processes. This resulted in a large increase in k_{rw} towards S2_N2 curve. Figure 3(a) compares the relative permeability curves for the drainage process.

The large increase in k_{rw} is due to the fact that there is less resistance to flow as pressure drops only occur in the throats resulting in a higher flow rate / conductivity for the wetting phase. Non-wetting phase (bulk) conductivity is dominated by the minimum inscribed radius in the flow path and thereby remains the same as the throat radius distributions are unchanged.

Thereafter, we replace the throat length distribution in S2_N3 with that of S2_N2 and re-simulate the displacement processes. The replacement of the throat length distribution is not possible for S1_N1 networks because it has a different number of nodes and throats. Figure 3(b, c and d) compares the relative permeability curves for the different

displacement processes for S2_N2 and S2_N3 networks and shows that both k_{rw} and k_{rnw} curves are in very good agreement (exactly on top of each other). This suggests / confirms that the large variations in k_{rw} are due to the differences in the geometrical characterization of the network elements.

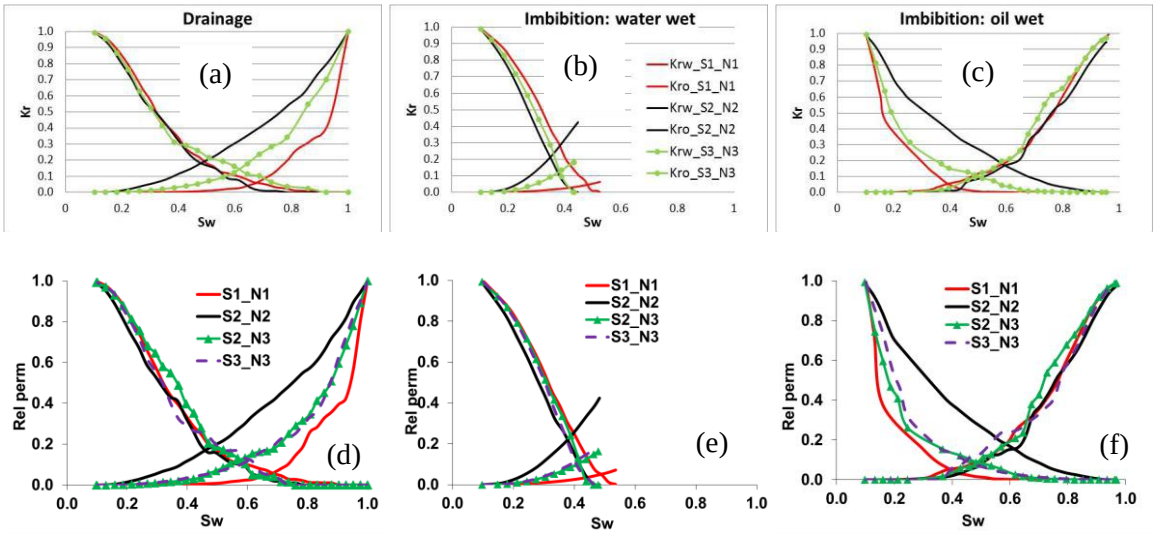

Figure 2**:** Comparison of published [1] relative permeability curves (a, b and c) with reproduced curves by using the e-Core code (d, e and f) for primary drainage, waterflooding at water-wet and oil-wet conditions respectively.

Comparison of relative permeability curves from S2_N3 and S3_N3, in Figure 2 (d, e and f) shows that both k_{rw} and k_{rnw} are approximately the same despite the fact that the networks are from different samples (S2 and S3) and have different number of pores, throats, etc. However, the networks have the same geometrical characterization (N3) and this further corroborates the consistency in relative permeability curves reported in [2]. It also confirms that the large variations in k_{rw} (reported for _N2 and _N3 networks) are due to differences in the geometrical characterization of the network elements.

COUNTER-INTUITIVE RELATIVE PERMEABILITY TRENDS

The conventional relative permeability trends expected for k_{rw} for different wettability conditions are that k_{rw} is lowest for water-wet, intermediate for mixed-wet and highest for oil-wet case and vice-versa for the k_{rnw} [15]. The published comparisons of imbibition relative permeability curves [1] for water-wet and oil-wet cases show however counter-intuitive trends for S2_N2 and S2_N3 networks while S1_N1 network shows the expected trend, Figure 4(a, b and c). Again, we first reproduce the published results as shown in Figure 4 (d, e and f) for the different wettability scenarios.

The total throat volume (summation of volumes in all the throats) in S2_N2 and S2_N3 networks is approximately 15% of the total pore space volume compared with 50% in S1_N1 network. While conserving total pore space volume, the total throat volume in

S2_N2 and S2_N3 is increased to 50% thereby reducing total pore bodies volume (summation of volumes in pore bodies) to 50%.

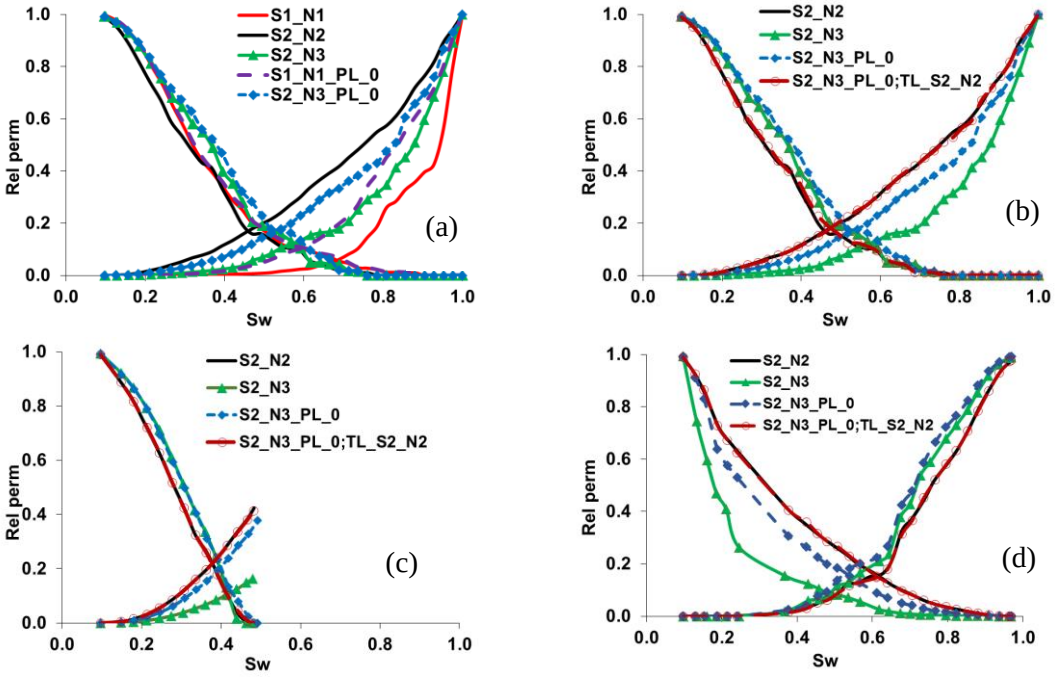

Figure 3: Comparison of original networks and modified networks (_PL_) relative permeability curves: (a) only pore lengths set to zero for primary drainage and (b), (c) and (d) where pore lengths are set to zero and the throat length of S2_N3 network replaced with that of S2_N2 network for primary drainage, waterflooding at water-wet and oil-wet conditions respectively.

Comparisons of the relative permeability trends from the networks with total throat volume of 15% (original networks) and 50% (modified networks) are shown in Figure 5. The trends change from counter-intuitive to the expected trends. Zhao *et al*. [3] also reported a counter-intuitive relative permeability trend for a sand pack network F with a porosity of 32.8% and permeability of 77,613 mD. Using the same approach, we examine a network extracted from a similar sand pack (F42B) with a porosity of 33.1% and permeability of 54,228 mD. The result is depicted in Figure 5(c) and shows that the relative permeability trend changes from counter-intuitive to the expected trend also by changing the total throat volume from 9% in the original network to 60% in the modified network.

For a better understanding of the effects that the total pore volume allocated to throat and pore elements have on relative permeability curves, we assign / allocate 15%, 30%, 50% and 75% of the total pore space volume to throats. Figure 6 compares the results for S2_N2 network. There is a consistent shift of the relative permeability curves and cross-over point to the right (increasing water saturation, S_w) as the percentage of the total pore volume allocated to throats increases.

This shift is due mainly to the change in saturation computation as more volume is allocated to throats and the primary drainage capillary pressure curves confirm this. At a given Pc value (for example at 5.0×10^{3} Pa in Figure 6(b)), the same throat has been invaded (since the throat radius distribution remains the same) but S_w changes from approximately 0.3 to 0.5 for networks where the total throat volume is 15% and 75% respectively. This progressive shift is also reflected in the waterflooding relative permeability curves as more volume is allocated to throats. However, the waterflooding end-point k_{rw} is the same for all cases as expected. This is depicted in Figure 6(c).

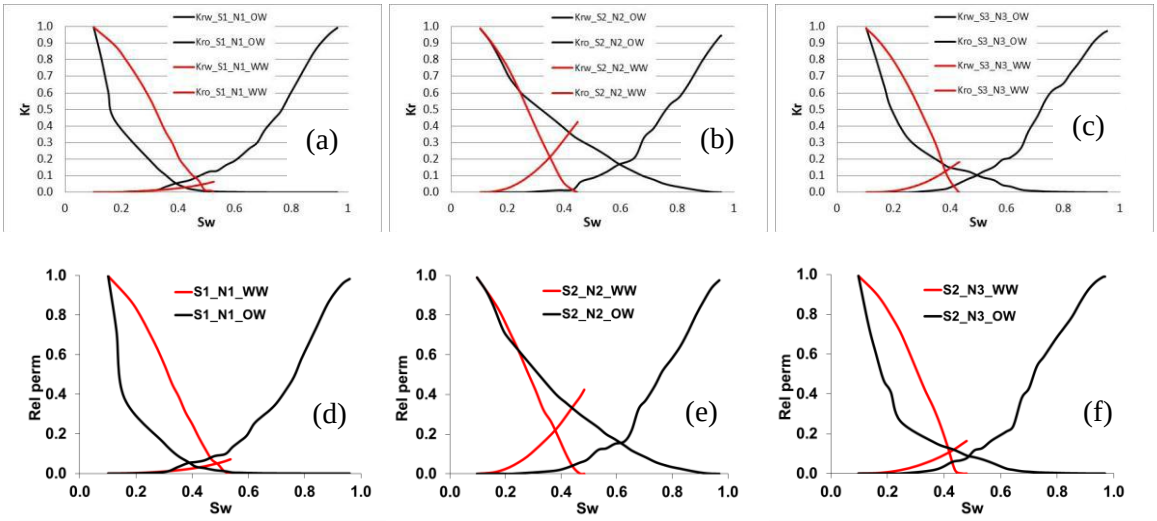

Figure 4**:** Comparison of published [1] relative permeability curves (a, b and c) with reproduced curves by using the e-Core code (d, e and f) for water-wet (WW) and oil-wet (OW) conditions.

REDUCING UNCERTAINTIES IN PORE NETWORK EXTRACTION PROCESSES

In real porous media, there is no demarcation of the pore space volume to throats and pores and the unanswered question is: what is the most reasonable percentage of total pore volume that should be allocated to throats? While this may be a tricky question as the percentage may vary with rock samples, we demonstrate below a simple technique of determining this by using a mercury injection $P_c - S_w$ curve simulated directly on the digitized image.

The injection of mercury into a digitized image of a sandstone reservoir rock sample with a porosity of 26.9% and permeability of 1,510 mD is simulated using a morphological approach [16] and $P_c - S_w$ curve is obtained. The pore space volume in the digitized image (grid) is not partitioned into pores and throats and hence no volume allocation is necessary. Next, we extract a network of pores and throats from the same image and determine the total volume allocated to throats and pores - 37% and 63% respectively. This network is referred to as the original network.

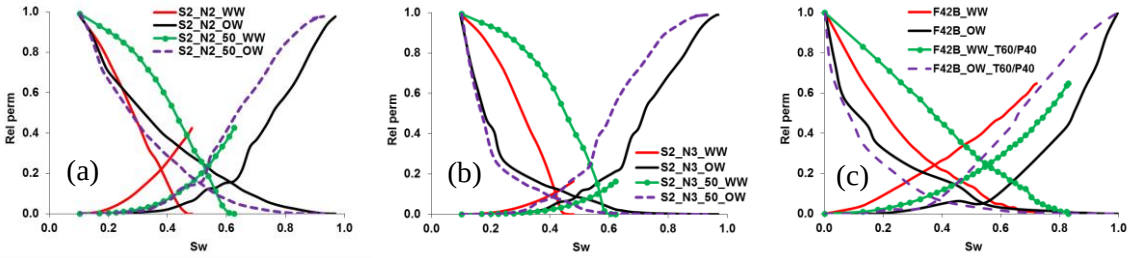

Figure 5**:** Comparison of the relative permeability trends for the original networks with 15% total pore volume in throats (TPVT) with modified network of 50% TPVT for (a) S2_N2 and (b) S2_N3 networks and (c) for a F42B sand pack network: the original network has 9% TPVT while the modified network has 60% TPVT.

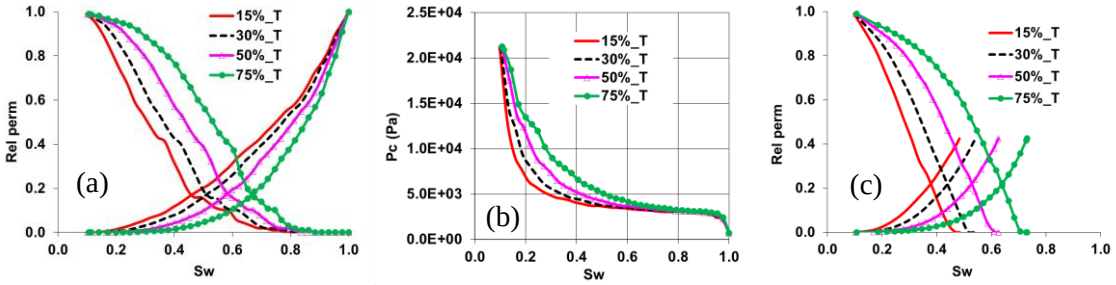

Figure 6: (a) primary drainage (PD) relative permeability curves, (b) PD capillary pressure curves and (c) waterflooding relative permeability curves at water-wet conditions for S2_N2 networks with different total pore volume allocated to throats

We then obtain modified networks from the original network by changing the total pore volume allocated to throats and pores to 15% and 85%; 50% and 50%; and finally 60% and 40% respectively. Oil/water primary drainage displacement is simulated on all the networks and the resulting oil/water $P_c - S_w$ curves are scaled into mercury/air $P_c - S_w$ curves using interfacial tensions and contact angles. The maximum Pc attainable from both the grid and network simulations is a function of the image resolution.

Figure 7 shows a comparison of the $P_c - S_w$ curves obtained on the grid with those from the original network and modified networks. It is obvious that the original network with total pore volume of 37% in throats provided the best match with the grid curve for this particular sample, Figure 7(b). The percentage will vary from one sample to another and this simple technique can be used to ascertain whether the allocated volume is reasonable or not.

CONCLUSIONS

The causes of apparent differences in predicted absolute permeability values, relative permeability curves and counter-intuitive relative permeability trends for the same sample as a result of differences in the extracted pore networks from digital rock images have been investigated. The estimated lengths for network elements (pores and throats) are responsible for the differences in the predicted transport properties for the networks examined in this study.

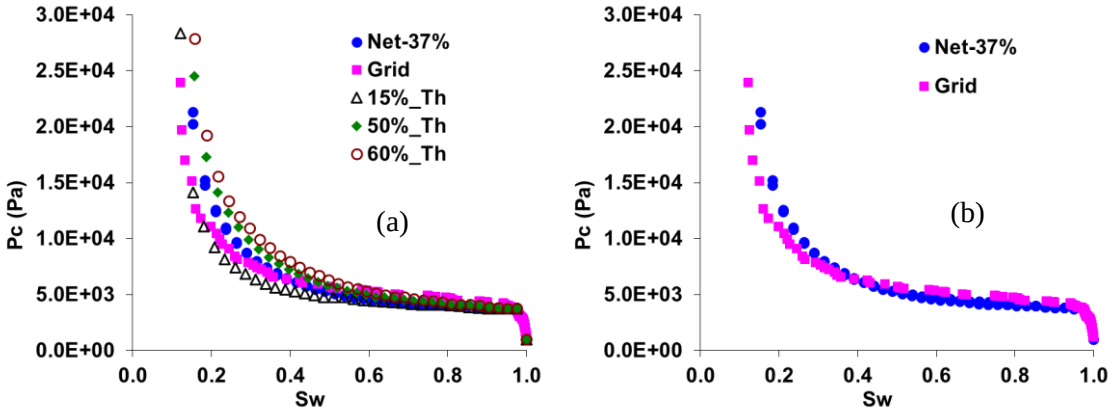

Figure 7: Comparison of Mercury injection $P_c - S_w$ curves obtained on a digitized image of a reservoir rock (Grid) with (a) those obtained from the original network (Net-37%) and modified networks with different total pore volume allocated to throats and (b) those obtained from the original network (Net-37%) only.

While there is no demarcation of the pore space volume to throats and pores in real porous media, this is required in pore network models. Using extracted networks from a Clashach sandstone sample and a sand pack, we show that volumes allocated to pores and throats during the pore network extraction processes are responsible for the observed counter-intuitive relative permeability trends reported recently in [1, 3].

Having understood the causes, we provide a simple but effective method of how some of the uncertainties associated with partitioning of the pore space into pores and throats during pore network extraction processes can be reduced using $P_c - S_w$ curves. This will ensure more representative pore networks, reduce differences in predicted transport properties and eliminate counter-intuitive trends in relative permeability curves without the requirement of experimental P_c data.

ACKNOWLEDGMENTS

The authors acknowledge Lithicon Norway AS for granting permission to publish this paper which is partly funded by RWE Dea and Norwegian Research Council through PETROMAKS Project Number: 208772/E30, titled: "Physically based three-phase relative permeability relations". We also thank STATOIL, TOTAL and Imperial College consortium on pore-scale modelling for sharing their samples and (or) data with us.

REFERENCES

1. Bondino, I., G. Hamon, W. Kallel, and D. Kachuma, "Relative permeabilities from simulation in 3D rock models and equivalent pore networks: critical review and way forward," SCA2012-01, *Proceedings of the International Symposium of the Society of Core Analysts*, Aberdeen, Scotland, UK (2012).
2. Idowu, N., C. Nardi, H. Long, and P.E. Øren, "Pore-Scale Modelling: Effects of Network Properties on Predictive Capabilities," SCA2012-35, *Proceedings of the*

International Symposium of the Society of Core Analysts, Aberdeen, Scotland, UK (2012).

3. Zhao, X., M.J. Blunt, and J. Yao, "Pore-scale modeling: Effects of wettability on waterflood oil recovery," *J. Pet. Sc. and Eng*., (2010) **71**, 169-178.
4. Hawkings, J. T., "Comparison of Three Methods of Relative Permeability Measurement," *The Log Analyst*, (1989) **30**, 5.
5. Amabeoku, M.O., F. Nakawaga, and R.H. BinNasser, "Quality Control/Quality Assurance Assessments of Core Analysis Data from Multiple Commercial Laboratories" *Proceedings of SPWLA 52nd Annual Logging Symposium*, Colorado, USA, (2011).
6. Ramstad, T., N. Idowu, C. Nardi, and P.E. Øren, "Relative permeability calculations from two-phase flow simulations directly on digital images of porous rocks," *Transport in Porous Media*, (2011) doi: 10.1007/s11242-011-9877-8.
7. Raeini, A.Q., M.J. Blunt and B. Bijeljic, "Modelling two-phase flow in porous media at the pore scale using the volume-of-fluid method," *J. Comp. Phys*., (2012), **231**, 5653-5668.
8. Sussman.,M., P. Smereka, and S. Osher, "A level set approach for computing solutions to incompressible two-phase flows," *J. Comp. Phys*. (1994), **114**, 146-159.
9. Meakin, P., and A.M. Tartakovsky, "Modeling and simulation of pore-scale multiphase fluid flow and reactive transport in fractured and porous media," *Rev. Geophys*. (2009), **47**, RG3002.
10. Øren, P.E., S. Bakke, and O.J. Arntzen, "Extending Predictive Capabilities to Network Models" *SPE Journal*, (1998), **3**, 324-336.
11. Valvatne, P.H., and M. Blunt, "Predictive pore-scale modeling of two-phase flow in mixed wet media," *Water Resources Research* (2004), 40, 1-21.
12. Zubair, K., S. Seraj, Z. Bhatti, A. Mock, P.E. Øren, V. Ravlo and O. Lopez, " Relative permeability assessment in a giant carbonate reservoir using Digital Rock Physics," SCA2012-03, *Proceedings of the International Symposium of the Society of Core Analysts*, Aberdeen, Scotland, UK (2012).
13. Øren P. E. and S. Bakke, "Process Based Reconstruction of Sandstones and Prediction of Transport Properties", *Transport in Porous Media*, (2002), **46**, 311-343.
14. Bhattad, P., C. S. Willson, and K.E. Thompson, "Effect of Network Structure on Characterization and Flow Modeling Using X-ray Micro-Tomography Images of Granular and Fibrous Porous Media," *Transport in Porous Media*, (2011), **90**, 363-391.
15. Anderson, W. G., "Wettability Literature Survey - Part 5: The Effects of Wettability on Relative Permeability", *Journal of Petroleum Technology*, (1987), 39, 1453-1468.
16. Vogel, H. J. J. Tölke, V. P. Schulz, M. Krafczyk, K. Roth, "Comparison of a Lattice-Boltzmann model, a Full Morphology Model, and a Pore Network Model for Determining Capillary Pressure-Saturation Relationships", *Vadose Zone Journal* **4** (2), 380–388.